IIETA International Information and Engineering Technology Association
Advancing the World of Information and Engineering

Instrumentation Mesure Métrologie
Vol. 25, No. 3, June, 2026, pp. 113-120
Journal homepage: http://iieta.org/journals/i2m

Polypropylene-Based Fiber Bragg Grating Temperature Sensors for Photovoltaic Monitoring

Dhay K. Hamdan*, Dina Yaqoob Matti

Department of Laser and Optoelectronics Engineering, College of Engineering, Al-Nahrain University, Baghdad 10072, Iraq

Corresponding Author Email: dhay.kadhim1988@nahrainuniv.edu.iq

https://doi.org/10.18280/i2m.250302

Received: 13 March 2026
Revised: 11 May 2026
Accepted: 21 May 2026
Available online: 26 June 2026

Keywords:
fiber Bragg grating, temperature sensor, photovoltaic monitoring, polypropylene substrate, Iraqi climate, solar cell efficiency

ABSTRACT

This paper presents a low-cost fiber Bragg grating (FBG) temperature sensor with a polypropylene substrate for real-time thermal monitoring of photovoltaic (PV) panels under harsh environmental conditions. The sensor exhibits thermal sensitivities of 70 pm/°C under simulated solar irradiance (≈1000 W/m²) and 74 pm/°C under laboratory conditions, representing a sevenfold improvement over bare FBG sensors (11 pm/°C), while remaining fully compatible with standard epoxy bonding methods. Over the operational temperature range of 55–80 °C, the sensor demonstrates excellent linearity ($R^2 > 0.99$), enabling reliable real-time measurement during PV panel operation. The potential of this technology in harsh environments, where the panel temperature can reach up to 75 °C and the ambient temperature reaches an even higher value as well, can be used in Middle Eastern climates, such as Iraq, where the ambient temperature is 50 °C or more, and the panel surface temperature is 80 °C or more.

1. INTRODUCTION

Photovoltaic (PV) generation is one of the most important renewable electricity supply options, particularly relevant for Iraq with its high solar irradiation levels. The global PV market is projected to reach the multi-terawatt scale by 2030, with silicon-based technologies expected to remain dominant [1]. However, an increased temperature of operation greatly reduces the efficiency of PV panels, in which performance decreases between 0.4 and 0.5% per °C above standard test conditions (25 °C) [2, 3]. Recent field studies on aged PV modules in harsh climates report annual degradation rates of 0.5–0.8% [4, 5], with thermal stress contributing substantially to long-term performance loss [4, 6]. However, maintaining PV systems under locally specific conditions is a great challenge to overcome, particularly in the Iraqi context, where maximum surface temperatures of ≥75 °C (tempered glass) and ambient temperatures exceed 50 °C [7, 8].

UV-induced solar cell damage and optical degradation dynamically shift thermal spots within field-modules, which also affects the long-term performance loss of modules in harsh desert climates [8, 9], and 23.3% reduction in maximum power is observed at full relevant environmental variation range after complete degradation analysis over a period of 25 years [10]. Combined impact of temperature and solar radiance leads to complex degradation phenomena, which must be monitored continuously to ensure optimum performance of the systems [11, 12]. The traditional temperature measurement technologies used in PV systems are susceptible to electromagnetic interference for conventional temperature sensing devices of PV monitoring were susceptible to harsh outdoor environment, and ultraviolet (UV) attacks will degrade their performance over time, as well as calibration drift problems [13]. Fiber Bragg grating (FBG) sensors possess distinguished characteristics like resistance to electromagnetic interference, high sensitivity, multiplexing capabilities, and long-term stability. Several recent comprehensive reviews have highlighted their broad applicability in structural health monitoring (SHM), aerospace and harsh environment sensing [14]. FBG-based temperature sensors are being developed with enhanced sensitivity by the design of a polymer-coated, substrate-assisted configuration [15]. The use of polymer encapsulation has been shown in several studies to significantly enhance the thermally induced strain transferred to the grating region. EpoCore-coated FBG sensors, for instance, have reached a sensitivity of up to 90.45 pm/°C by optimizing UV exposure and post-curing conditions [16].

Polymer-coating FBGs have also been reported for cryogenic temperature monitoring, showing sensitivity of 48 pm/°C [17]. Also, thermosetting epoxy systems tuned to the aerospace environment led to a sensitivity of 26.6 pm/°C [18]. Moreover, flexible polymer materials like PDMS have facilitated mechanically compliant FBG sensors, culminating in tensile displacement sensitivities of up to 3.69 nm/mm for potential uses in wearable and gesture-recognition applications [19]. But most sensitivity optimization techniques depend on complex fabrication processes and specific infrastructure, like UV curing systems or precision tapering setups, along with numerical optimization tools like ANSYS (commercial simulation software for thermal and structural analysis), which make the process much more expensive and challenging in large-scale implementation. Nonetheless, despite these technical difficulties, recent research has

validated the robustness of FBG sensors in extreme operating conditions. For example, embedded FBG sensors inside Carbon Fiber Reinforced Polymer (CFRP) optical bench structures were shown to perform consistently in space-relevant operating conditions [20]. Likewise, there are large-scale road surface monitoring applications in which distributed and multi-point FBG arrays have successfully been implemented [21, 22]. Importantly, in extreme environments, temperature measurement is vital for PV systems; yet conventional sensing techniques suffer to some extent from electromagnetic interference, calibration drift and UV-induced degradation. Although FBG sensors are mature technology with electromagnetic interference immunity and inherent thermal stability, the low optical response ~11 pm/°C [23] still needs precise methods to enhance the sensitivity. The polymer-enhanced FBG sensors presently developed have exhibited increased sensitivity; nevertheless, they require complicated fabrication processes with specialist equipment like UV curing machines, precision taper making systems and numerical optimization tools that would be difficult to utilize on-site at scarce resource locations. Results are increasingly supporting the fact that FBG-based sensing is mature enough for deployment in harsh environments. However, efficient low-cost and sensitive FBG temperature sensors suitable specifically for PV monitoring in extreme climate applications and production process simplicity that is compatible with mass production are still required. Here we fill this gap by demonstrating that bond formation on polypropylene substrates using proven epoxy adhesive can yield competitive thermal sensitivity (74 pm/°C) while leveraging already established fabrication infrastructure.

The applied nature of this work is where the incremental contribution lies. It specifically investigates the application of FBG sensors for monitoring temperature and assessing the condition of PV panels instantaneously. In this regard, the present contribution goes beyond a standard application of FBG as a temperature sensor and proposes its adoption as an integrated sensing element that improves monitoring performance and operation reliability of PV systems. The suggested implementation is cost-effective and straightforward from a practical point of view. Then, the polypropylene substrates have an approximate mass of about 0.7 g. Also, there was used in a small quantity (less than 1 g) of epoxy adhesive was used. The unit cost of the proposed system modifications is around 0.04 USD. In addition, the design process is simple (approximately 4 minutes) and does not impose any complexity, thus reflecting on both feasibility and ease of deployment for the proposed approach.

The rest of the paper is structured as follows: Section 2 provides theoretical background; Section 3 describes experimental methodology; Section 4 presents the results and discussion, including subsections on bare FBG response, PP-bonded FBG characterization, repeatability, and comparative analysis. The conclusion is drawn in Section 5.

2. THEORETICAL BACKGROUND

The subject of this work is based on two pillars that constitute the theoretical background: the PV cells' temperature dependence and the theory of operation of FBG sensors and their enhancement mechanisms. The increased intrinsic carrier concentration and decreased open-circuit voltage according to the relation $VOC(T) = VOC(T_0) - \beta VOC\,(T - T_0)$, where βVOC is the voltage temperature coefficient (ranging from 2.2 to 2.4 mV/°C per cell), T is the operating temperature of the solar cell and T_0 is the reference temperature. This results in efficiency reductions of 0.3–0.5% per °C above 25 °C and an approximately 15% power loss at 60 °C [24, 25]. FBG sensors are wavelength-selective reflectors that are created by a periodic modulation of refractive index along the direction of the fiber core [26], with the Bragg wavelength defined as $\lambda_B = 2n_{eff}\,\Lambda$ [27], where λ_B is the nominal Bragg wavelength (nm), n_{eff} is the effective refractive index of the guided mode, and Λ is the grating period. The thermally induced wavelength shift is expressed as $\Delta\lambda_B / \lambda_B = (\alpha f + \xi)\,\Delta T$, where $\alpha f \approx 0.55 \times 10^{-6}$ °C^{-1} is the thermal expansion coefficient describing the physical elongation of the fiber with temperature [28], and $\xi \approx 6.67 \times 10^{-6}$ °C^{-1} is the thermo-optic coefficient describing the change in refractive index with temperature [29]; together these yield a baseline sensitivity on the order of 10–11 pm/°C for a bare FBG centered near 1550 nm [30], when a tension is exerted from the outside, we add a photo-elastic correction term and then obtain the full fractional shift as $\Delta\lambda_B / \lambda_B = (1 - Pe)\,\Delta\varepsilon + (\alpha f + \xi)\,\Delta T$ [31], where $Pe \approx 0.22$ is the effective photo-elastic coefficient of silica, accounting for the portion of the refractive index change induced by mechanical strain, and $\Delta\varepsilon$ is the applied mechanical strain. When the FBG is bonded to a substrate whose thermal expansion coefficient αsub significantly exceeds that of silica, such as polypropylene with $\alpha PP \approx 100–150 \times 10^{-6}$ °C^{-1} [31], the substrate expands more rapidly upon heating and applies an additional elastic strain to the fiber, yielding a net temperature sensitivity of $\Delta\lambda_B / \Delta T = \lambda B\,[(\alpha f + \xi) + (1 - Pe)\,\eta\,(\alpha sub - \alpha f)]$ [32, 33], where αsub is the thermal expansion coefficient of the substrate material, and $\eta\,(0 \le \eta \le 1)$ is the strain transfer efficiency from the substrate to the fiber, which approaches unity when a stiff, thin adhesive layer is used. Consequently, the greater the mismatch $(\alpha sub - \alpha f)$, the higher the achievable sensitivity enhancement. This principle governs the polypropylene-bonded FBG sensor configuration investigated in this study, which achieved a sensitivity of approximately 70–75 pm/°C.

3. EXPERIMENTAL METHODOLOGY

As shown in Figure 1, a laboratory-scale optical, thermal, and PV measurement system was built using commercial fiber-optic instruments and a custom solar simulator designed to replicate harsh climatic conditions, such as natural Iraqi sunlight.

Optical excitation of the FBG sensor was provided by a broadband amplified spontaneous emission (ASE) source (HITASE-M-C-20-N-FA) operating in the C-band spectral range of 1528–1566 nm with a stable output optical power of 20 mW, delivered through single-mode fiber terminated with FC/APC connectors to suppress Fresnel back-reflections.

Optical signal routing between the light source, the FBG sensor, and the detection unit was achieved using a three-port optical circulator (PICIR-3-1550), optimized for 1550 nm operation with a ±30 nm bandwidth, insertion loss below 2 dB, isolation exceeding 28 dB, and full compatibility with SMF-28 fiber and FC/APC interfaces. This arrangement provided for one-way light travelling to the sensing element, and direct redirection of the reflected Bragg signal with low directivity to the interrogating head with minimal optical feedback.

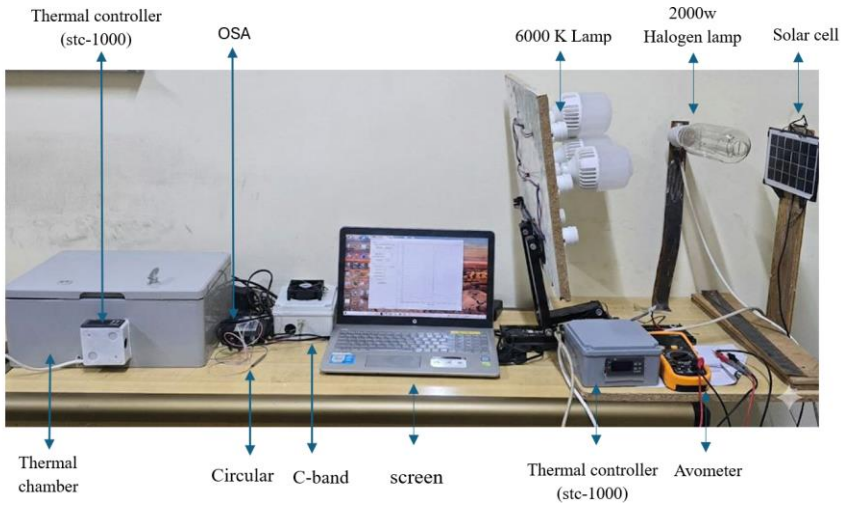

Figure 1. Schematic diagram of the laboratory-based solar simulation system showing the arrangement of 6000 K lamps, halogen source, and photovoltaic (PV) cell with fiber Bragg grating (FBG) sensor attachment and thermal chamber

The reflection FBG spectrum was acquired by an optical spectrum analyzer OSA (HITOSA-M-C-FA), providing a wavelength measurement of 1527 nm to 1565 nm, wavelength repeatability of ±2 pm, spectral resolution of less than 2 pm, and detectable −75 dBm to +5 dBm. The device can detect very small thermally induced Bragg wavelength shifts.

To assess sensors' performance under simulated outdoor conditions, a laboratory-size solar simulator was assembled by using three high-luminance white LED6000 K (for two lamps) and a single halogen lamp of 2000 W/220 V, following standard solar simulator development practices. The system was modified to simulate Earth's diffuse ambient radiative flux, giving an irradiance of 1000 W/m² and an illumination level of about 110,000 lux, measured by a calibrated digital illuminometer (LX-1010 B).

The PV under consideration was a polycrystalline silicon solar cell with dimensions of 13 cm × 25 cm. Its electrical performance was measured with a precision digital multimeter to record PV output voltage under different irradiance and temperature values. Surface temperature was monitored using a calibrated digital thermometer and an STC-1000 temperature controller.

For controlled thermal characterization, the FBG sensor assembly was evaluated inside a thermal chamber regulated by the same STC-1000 controller and a 100 W tungsten lamp heat source, with temperature varied from 55 °C to 80 °C in 5 °C increments and independently verified using a calibrated thermocouple with an accuracy of ±0.5 °C.

Commercial short-period FBG sensors were employed, featuring a nominal Bragg wavelength of 1550 ± 0.3 nm, a full width at half maximum below 0.3 nm, a side-mode suppression ratio exceeding 15 dB, reflectivity greater than 90%, and a grating length of 10 mm. The gratings were inscribed in standard SMF-28e single-mode optical fiber with intact acrylate coating over the grating region and a total pigtail length of 2 m.

For enhanced thermal strain transfer, as shown in Figure 2, the FBG sensor was bonded to a polypropylene substrate with dimensions of 4 cm × 0.5 cm × 4 mm using a fast-curing two-part epoxy adhesive (4-minute epoxy, 1:1 mixing ratio), achieving full mechanical curing after 24 hours and forming a stiff, stable joint that ensured efficient strain coupling between the substrate and the FBG sensor. Despite the low intrinsic thermal conductivity of polypropylene, the resulting sensor assembly provided reliable, repeatable, and consistent temperature measurements under both controlled and simulated outdoor operating conditions.

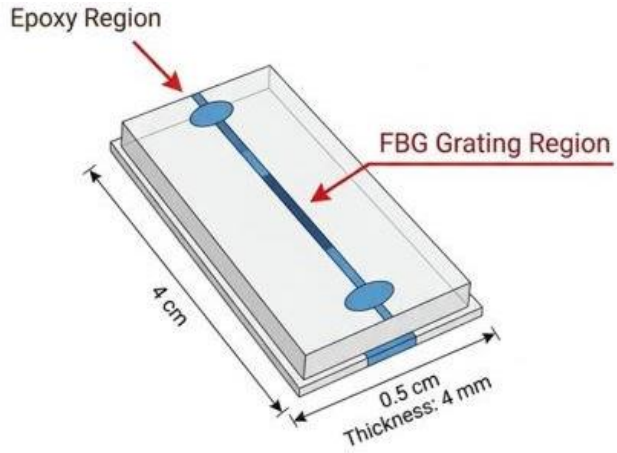

Figure 2. Fiber Bragg grating (FBG) sensor bonded to a polypropylene substrate

4. RESULTS AND DISCUSSION

4.1 Bare FBG thermal and photovoltaic response

As seen in Figure 3, the thermal response of a bare (unbonded) FBG, serving as a reference baseline the Bragg wavelength exhibits a linear variation with temperature, ranging from 1550.188 nm at 45 °C to 1550.530 nm at 75 °C, resulting in a correlation coefficient of $R^2 = 0.99929$ and approximately a temperature sensitivity of approximately 11 pm/°C, which confirmed impressive linearity and reproducibility of thermal response of proposed FBG. This change is attributed to the combined action of thermo-optic effect (change in index of refraction with temperature) and thermal expansion of the silica, which increases the effective period of the grating and consequently its Bragg reflected wavelength.

Figure 4 presents the variation of PV voltage (V, volts) versus temperature (T, °C), all under the same experimental conditions. The photo-voltaic voltage shows a clear inverse

relationship with temperature, decreasing in a linear form from 7.54 V at 45 °C to 6.89 V at 75 °C (linear fit: $R^2 = 0.99929$ and the slope is -0.0213 V/°C, indicating that open-circuit voltage decreases with an increase in temperature, which is already a well-known thermal characteristic for silicon-based solar cells).

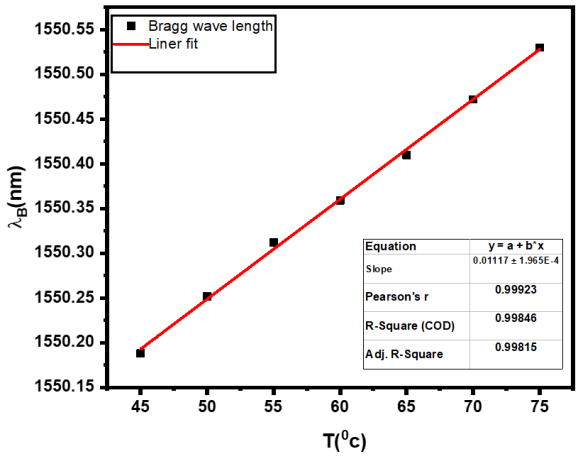

Figure 3. Temperature dependence of Bragg wavelength and photovoltaic (PV) of the bare fiber

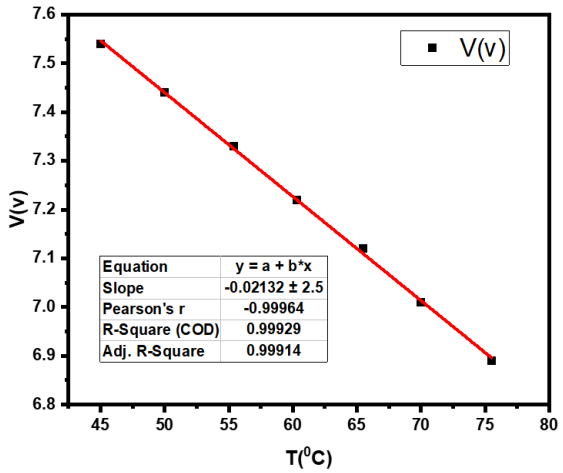

Figure 4. Variation of photovoltaic (PV) voltage with temperature for the bare fiber

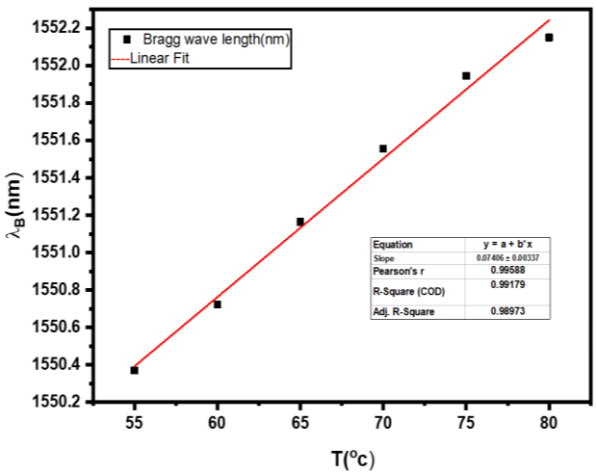

Figure 5. Thermal response of a polypropylene-bonded fiber Bragg grating (FBG) sensor in a controlled thermal chamber

4.2 PP-bonded FBG in thermal chamber

Figure 5 shows the thermal behavior of an FBG sensor attached to a polypropylene substrate and measured in a thermal chamber. The Bragg wavelength is linearly red-shifted with the temperature, attributed to the thermal expansion–induced thermo-optic effect of the silica fiber together with that induced by the strain from the polymer substrate. The extracted thermal sensitivity of 74 pm/°C corresponds to its intrinsic effective sensitivity from an FBG–polymer system under homogeneous and stationary thermal conditions. The high linearity, which is verified by the Pearson correlation coefficient and the determination factor (R^2), indicates good strain transfer and excellent sensor output, offering a well-calibrated baseline.

4.3 PP-bonded FBG on operational solar cell

Figure 6 demonstrates the thermal performance of the same polypropylene-bonded FBG sensor when attached to a solar cell. When compared to the sensitivity obtained in a thermal chamber environment, the measured value decreases to ~70 pm/°C, mirroring practical effects. These effects include actual thermal interface resistance and some strain relaxation within the adhesive–substrate–cell assembly, where it is confined to one location.

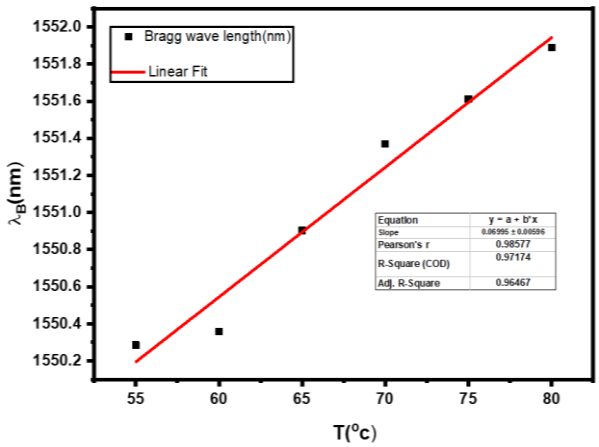

Figure 6. Operational thermal monitoring of a solar cell using a polypropylene-bonded fiber Bragg grating (FBG) sensor

Figure 7 shows the reflection spectra of the FBG sensor measured at 60 °C, 70 °C, and 80 °C. A clear red shift of the Bragg wavelength is observed with increasing temperature, indicating a linear thermal response of the FBG sensor. This wavelength shift is attributed to the combined thermo-optic effect and thermal expansion of the fiber, confirming the suitability of the sensor for temperature monitoring.

4.4 Repeatability and measurement uncertainty

We performed three independent measurements of alternating heating-cooling cycles for each case (thermal chamber and solar simulator) to assess repeatability and stability of the measurements. The Bragg wavelength was measured at each temperature setpoint and the temperature sensitivity was derived from linear regression of λ_B against temperature for each cycle. The measured sensitivities were the average ± standard deviation of the sensitivities obtained

from the three cycles. The average sensitivity recorded in the thermal chamber was 74 ± 1 pm/°C and under the solar simulator, it was 70 ± 2 pm/°C. The small standard deviation reflects the stability of the measurement, with less than 3% variation from cycle to cycle. The measurements were performed using a single FBG sensor sample, and the reported values are the average performance of this device over multiple measurements. The results are illustrated in Figures 5 and 6.

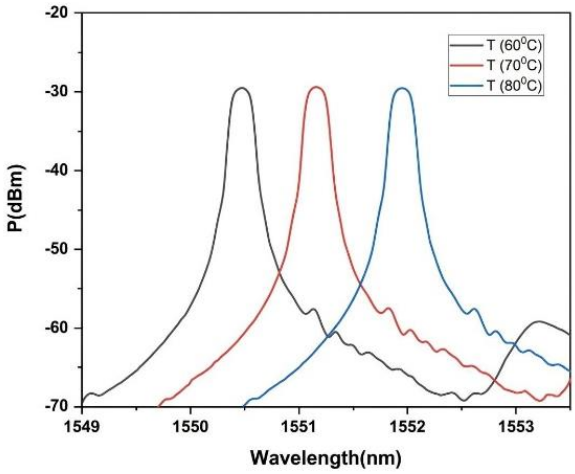

Figure 7. Reflection spectra of the fiber Bragg grating (FBG) sensor at different temperatures

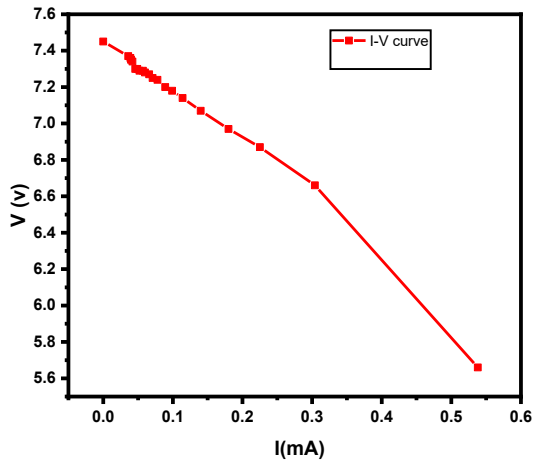

Figure 8. Current-voltage (I-V) characteristics of the solar cell at 30 °C under 1000 W/m² irradiance

The experiment was set up with an ammeter in series with the solar cell and a variable resistor (10–200 Ω) and a voltmeter across the cell terminals. The solar irradiance was kept at around 1000 W/m² by using a lux meter and the temperature was kept at 30 C by using an STC-1000 controller to maintain a constant condition. The operating point was changed by changing the load resistance every ten degrees, to be close to short-circuit conditions (high current, low voltage) to open-circuit conditions, at which point the voltage was 7.45 V and the current was near zero. The current measured at 0.538 A at 10 Ω dropped to 0 A at no load. Using these measurements, a representative current-voltage (I-V) curve was obtained, which has the desired nonlinear behavior with a distinct maximum power region. The highest recorded output power was about 3.04 W with a load resistance of 10 Ω. The derived I-V curve is a sufficient model of the electrical performance of the PV cell under controlled conditions and is adequate to the extent of this study, as shown in Figure 8.

As shown in Table 1, the polypropylene-bonded FBG has higher sensitivity and good linearity.

Table 1. Experimental results summary of polypropylene-bonded fiber Bragg grating (FBG) temperature sensor

Parameter	Bare FBG	Polypropylene-Bonded FBG (Thermal Chamber)	Polypropylene-Bonded FBG (Solar Cell)
Temperature Range (°C)	45–75	55–80	55–80
Sensitivity (pm/°C)	11	74 ± 1	70 ± 2
Linearity (R^2)	0.99929	>0.9918	>0.99
Enhancement Factor	1× (baseline)	7×	6.4×
Testing Condition	Thermal chamber	Thermal chamber	Under solar irradiance (1000 W/m²)

4.5 Discussion

The linearity of the response throughout the whole measurement range was verified by a high coefficient of determination ($R^2 > 0.9918$), proving that the polypropylene-bonded FBG substrate sensor has linear behavior and stable performance, which is suitable for PV applications in practice.

The slight decrease in sensitivity observed under operational conditions underscores the importance of calibrating all measuring instruments under controlled conditions before field deployment, while also confirming that polymer-bonded fiber grating sensors are capable of detecting temperature changes and heat build-up in solar cells. The wavelength response of the FBG-polypropylene sensor was found to be a linear function of temperature across the full measurement range. The thermal chamber measurements were done in the range of 55–80 °C, which was chosen to simulate real operating conditions for PV panels in the Iraqi environment where ambient temperatures can be greater than 50 °C and the solar cell surface temperature exposed to a direct solar irradiance can reach up to ~75 °C; this range is suitable for initially capturing thermal anomalies that commonly occur with devices placed in operations such as cell degradation hotspots associated with areas of partial shading or junction breakdown. In addition to that, this range guarantees the thermal stability of epoxy-polypropylene bonding while also providing a broad linear operating interval that can be considered as an effective but dependable one. Under laboratory conditions, a 74 pm/°C sensitivity was obtained with $R^2 > 0.9918$ linearity coefficient upon being assessed against an operational solar cell at irradiance levels ≈1000 W/m², the identified sensitivity was recorded to be 70 pm/°C, or a decrease of 5.4% owing to thermal interface resistance and localized heat dissipation occurring within the assembly of cell-substrate. The obtained sensitivity of 74 pm/°C is an excellent 7-fold improvement over the theoretical baseline performance limit of bare FBG sensors, which has been estimated to be 11 pm/°C. Such enhancement is attributed to the large thermal expansion coefficient of polypropylene ($100–150 \times 10^{-6}$ $°C^{-1}$) that aids in transferring thermally induced stress into the optical fiber through the epoxy adhesive layer. Excellent linearity and repeatability over several

thermal cycles provide evidence for the mechanical stability of the epoxy-substrate-fiber assembly, supporting its suitability for long-term operation under load.

Table 2 presents a comprehensive comparison of the polypropylene-enhanced FBG sensor developed in this study with recent polymer-based enhancement methods reported in the literature. The analysis shows that while certain methods achieve higher absolute sensitivity, such as EpoCore-coated FBG sensors reaching 90.45 pm/°C the proposed polypropylene-epoxy approach offers a favorable tradeoff between thermal sensitivity and practical applicability, requiring no specialized fabrication equipment. The sensitivity of 74 pm/°C was achieved using standard fabrication techniques, making it accessible with common materials and can be processed at room temperature.

Unlike dedicated tools, such as UV cure tools, precision tapering and cryogenic testing facilities, the new sensor can be fabricated easily from readily available parts and cured at a much higher temperature than conventional epoxy bonding, making it well-suited for widespread use in resource-constrained environments. Operational validation with simulated solar irradiance (1000 W/m²) retaining a sensitivity of 70 pm/°C, at the same time, proves that it is fit for use under harsh conditions. PV monitoring operations outside, especially at high temperatures and UV irradiation, require both good performance properties and long-term reliability.

Table 2. Comparison of polymer-enhanced fiber Bragg grating (FBG) temperature sensors

Polymer Material	Sensitivity (pm/°C)	Temp. Range (°C)	Application	Fabrication	Key Features	Ref.
EpoCore, 2025	90.45	−20–100	Power equipment	UV + thermal cure	9× bare, insulated	[16]
Polymer (PCFBG), 2018	48	−196–25	Cryogenic composites	Polymer coating	10× bare FBG	[17]
Epoxy Thermosetting, 2024	26.6	80–270	Aerospace cryogenic	Capillary recoating	$R^2 = 0.997$ linearity	[18]
PDMS (Wearable), 2024	3.69 nm/mm	−45–200	Gesture recognition, health monitoring	Embedded in an elastomer	Biocompatible, <6% hysteresis	[19]
Polyimide, 2023	11 pm/°C	Space-relevant range	Structural health monitoring (SHM), humidity	Embedded in CFRP	Thermal stability up to 300 °C, space-qualified	[20]
Polypropylene + Epoxy (this work), 2025	74/70	55–85	Solar panel monitoring	Standard + epoxy	7× bare, low cost	Proposed

5. CONCLUSIONS

This paper presents a low-cost, high-sensitivity FBG temperature sensor constructed on a polypropylene substrate for PV panel temperature monitoring under extreme environmental conditions.

The main results and contributions are as follows:

- A substantial enhancement in thermal sensitivity was demonstrated under both controlled and operational conditions, representing a seven-fold improvement over a bare FBG sensor (11 pm/°C).
- Excellent linearity ($R^2 > 0.99$) was obtained over the temperature range of 55–80 °C, making the sensor suitable for transient measurements.
- The sensitivity exceeds or is at least comparable to that of previously reported polymer-enhanced FBG sensors.
- Fabrication complexity is reduced by using common materials and room-temperature processing methods, making the sensor suitable for mass production.

The demonstrated performance positions this sensor for several promising applications, particularly in PV plants located in harsh climatic regions where ambient temperatures exceed 50 °C and panel surface temperatures can reach above 75 °C. Additional potential uses include cost-effective outdoor monitoring in underdeveloped areas, the deployment of distributed sensor arrays to obtain accurate thermal maps across entire PV plants, and integration into early warning systems for hotspot detection (as future work). Key directions for future work comprise long-term field validation over 12 months and under more than 1000 thermal cycles; assessment of UV resistance and development of a protective coating; investigation of alternative high-temperature substrates to extend the operating range beyond 80 °C; multiplexed nano-based sensor array mapping; wireless connectivity for autonomous operation; and establishment of manufacturing protocols and calibration standards.

These results bridge the gap in PV temperature sensing technology by demonstrating that ultra-high sensitivity can be achieved through simple and low-cost fabrication methods, potentially enabling widespread adoption of fiber optic sensing in large-scale renewable energy systems, particularly in developing regions where harsh environmental conditions and limited resources call for practical, reliable and affordable monitoring solutions.

REFERENCES

[1] Haegel, N.M., Verlinden, P., Victoria, M., Altermatt, P., et al. (2023). Photovoltaics at multi-terawatt scale: Waiting is not an option. Science, 380(6640): 39-42. https://doi.org/10.1126/science.adf6957

[2] Green, M.A., Hishikawa, Y., Dunlop, E.D., Levi, D.H., Hohl-Ebinger, J., Ho-Baillie, A.W.Y. (2018). Solar cell efficiency tables (version 52). Progress in Photovoltaics: Research and Applications, 26(7): 427-436. https://doi.org/10.1002/pip.3040

[3] Gasparin, F.P., Kipper, F.D., de Oliveira, F.S., Krenzinger, A. (2022). Assessment on the variation of temperature coefficients of photovoltaic modules with solar irradiance. Solar Energy, 244: 126-133. https://doi.org/10.1016/j.solener.2022.08.052

[4] Rajput, P., Singh, D., Singh, K.Y., Karthick, A., Shah, M.A., Meena, R.S., Zahra, M.M.A. (2024). A comprehensive review on reliability and degradation of

PV modules based on failure modes and effect analysis. International Journal of Low-Carbon Technologies, 19: 922-937. https://doi.org/10.1093/ijlct/ctad106

[5] Daher, D.H., Aghaei, M., Quansah, D.A., Adaramola, M.S., Parvin, P., Ménézo, C. (2023). Multi-pronged degradation analysis of a photovoltaic power plant after 9.5 years of operation under hot desert climatic conditions. Progress in Photovoltaics: Research and Applications, 31(9): 888-907. https://doi.org/10.1002/pip.3694

[6] Torki, Z., Benhamida, M., Haddad, Z., Nahoui, A., Chouder, A., Brahimi, I. (2024). Effects of temperature and solar radiation on photovoltaic modules performances installed in Oued Keberit Power Plant, Algeria. Journal of Advanced Research in Fluid Mechanics and Thermal Sciences, 112: 204-216. https://doi.org/10.37934/arfmts.112.1.204216

[7] Hassan, Q., Hafedh, S.A., Hasan, A., Jaszczur, M. (2022). Evaluation of energy generation in Iraqi territory by solar photovoltaic power plants with a capacity of 20 MW. Energy Harvesting and Systems, 9(1): 97-111. https://doi.org/10.1515/ehs-2021-0075

[8] Al-Ghezi, M.K., Ahmed, R.T., Chaichan, M.T. (2022). The influence of temperature and irradiance on performance of the photovoltaic panel in the middle of Iraq. International Journal of Renewable Energy Development, 11(2): 501. https://doi.org/10.14710/ijred.2022.43713

[9] Segbefia, O.K. (2023). Temperature profiles of field-aged photovoltaic modules affected by optical degradation. Heliyon, 9(9): e19566. https://doi.org/10.1016/j.heliyon.2023.e19566

[10] Atia, D.M., Hassan, A.A., El-Madany, H.T., Eliwa, A.Y., Zahran, M.B. (2023). Degradation and energy performance evaluation of mono-crystalline photovoltaic modules in Egypt. Scientific Reports, 13(1): 13066. https://doi.org/10.1038/s41598-023-40168-8

[11] Sepulveda-Oviedo, E.H. (2025). Impact of environmental factors on photovoltaic system performance degradation. Energy Strategy Reviews, 59: 101682. https://doi.org/10.1016/j.esr.2025.101682

[12] Afonso, D., Mesbahi, O., Bouich, A., Tlemçani, M. (2025). Influence of long-term and short-term solar radiation and temperature exposure on the material properties and performance of photovoltaic panels: A comprehensive review. Energies, 18(19): 5072. https://doi.org/10.3390/en18195072

[13] Dhanalakshmi, S., Chakravartula, V., Narayanamoorthi, R., Kumar, R., Dooly, G., Duraibabu, D.B., Senthil, R. (2022). Thermal management of solar photovoltaic panels using a fibre Bragg grating sensor-based temperature monitoring. Case Studies in Thermal Engineering, 31: 101834. https://doi.org/10.1016/j.csite.2022.101834

[14] Alhussein, A.N., Qaid, M.R., Agliullin, T., Valeev, B., Morozov, O., Sakhabutdinov, A. (2025). Fiber Bragg grating sensors: Design, applications, and comparison with other sensing technologies. Sensors, 25(7): 2289. https://doi.org/10.3390/s25072289

[15] Alshaikhli, Z.S. (2024). A comparative study on polymer and metals coated TFBG temperature sensor: Coating thickness impact. Applied Physics A, 130(2): 127. https://doi.org/10.1007/s00339-023-07269-7

[16] Li, Q., Li, Y.C., Shao, J., Wang, T.L., et al. (2024). Research on temperature sensitivity of FBG sensor based on EpoCore adhesive coated. Opto-Electronic Engineering, 51(12): 240228. https://doi.org/10.12086/oee.2024.240228

[17] Sampath, U., Kim, D., Kim, H., Song, M. (2018). Polymer-coated FBG sensor for simultaneous temperature and strain monitoring in composite materials under cryogenic conditions. Applied Optics, 57(3): 492-497. https://doi.org/10.1364/AO.57.000492

[18] Ren, Y., Song, H., Cai, Q., Cai, Z., Liu, Y., Wang, B. (2024). Modeling analysis and experimental study on epoxy packaged FBG sensor for cryogenic temperature measurement. Optical Fiber Technology, 84: 103710. https://doi.org/10.1016/j.yofte.2024.103710

[19] Xiao, K., Wang, Z., Ye, Y., Teng, C., Min, R. (2024). PDMS-embedded wearable FBG sensors for gesture recognition and communication assistance. Biomedical Optics Express, 15(3): 1892-1909. https://doi.org/10.1364/BOE.517104

[20] Fernández-Medina, A., Frövel, M., López Heredero, R., Belenguer, T., de la Torre, A., Moravec, C., San Julián, R., Gonzalo, A., Cebollero, M., Álvarez-Herrero, A. (2023). Embedded fiber Bragg grating sensors for monitoring temperature and thermo-elastic deformations in a carbon fiber optical bench. Sensors, 23(14): 6499. https://doi.org/10.3390/s23146499

[21] Braunfelds, J., Senkans, U., Skels, P., Janeliukstis, R., Porins, J., Spolitis, S., Bobrovs, V. (2022). Road pavement structural health monitoring by embedded fiber-Bragg-grating-based optical sensors. Sensors, 22(12): 4581. https://doi.org/10.3390/s22124581

[22] Kashaganova, G., Kozbakova, A., Kartbayev, T., Togzhanova, K., Alimseitova, Z., Sergazin, G. (2024). Design of a fiber temperature and strain sensor model using a fiber Bragg grating to monitor road surface conditions. Inventions, 9(5): 100. https://doi.org/10.3390/inventions9050100

[23] Song, Z., Wang, M., Payne, F.P., Salter, P.S., Liu, T., Elston, S.J., Booth, M.J., Morris, S.M., Fells, J.A. (2025). Fiber Bragg gratings with micro-engineered temperature coefficients. Advanced Optical Materials, 13(8): 2402726. https://doi.org/10.1002/adom.202402726

[24] Varshni, Y.P. (1967). Temperature dependence of the energy gap in semiconductors. Physica, 34(1): 149-154. https://doi.org/10.1016/0031-8914(67)90062-6

[25] Singh, P., Ravindra, N.M. (2012). Temperature dependence of solar cell performance—An analysis. Solar Energy Materials and Solar Cells, 101: 36-45. https://doi.org/10.1016/j.solmat.2012.02.019

[26] Theodosiou, A. (2024). Recent advances in fiber Bragg grating sensing. Sensors, 24(2): 532. https://doi.org/10.3390/s24020532

[27] Kok, S.P., Go, Y.I., Wang, X., Wong, M.D. (2024). Advances in fiber Bragg grating (FBG) sensing: A review of conventional and new approaches and novel sensing materials in harsh and emerging industrial sensing. IEEE Sensors Journal, 24(19): 29485-29505. https://doi.org/10.1109/JSEN.2024.3434351

[28] Zhao, X., Wei, C., Zeng, L., Sun, L., et al. (2024). Research progress in fiber Bragg grating-based ocean temperature and depth sensors. Sensors, 25(1): 183. https://doi.org/10.3390/s25010183

[29] Erdogan, T. (1997). Fiber grating spectra. Journal of Lightwave Technology, 15(8): 1277-1294.

https://doi.org/10.1109/50.618322
[30] Yassin, M.H., Farhat, M.H., Soleimanpour, R., Nahas, M. (2024). Fiber Bragg grating (FBG)-based sensors: A review of technology and recent applications in structural health monitoring (SHM) of civil engineering structures. Discover Civil Engineering, 1(1): 151. https://doi.org/10.1007/s44290-024-00141-4
[31] Khina, A.G., Bulkatov, D.P., Storozhuk, I.P., Sokolov, A.P. (2025). Coefficient of linear thermal expansion of polymers and polymer composites: A comprehensive review. Polymers, 17(23): 3097. https://doi.org/10.3390/polym17233097
[32] Qin, H., Tang, P., Lei, J., Chen, H., Luo, B. (2023). Investigation of strain-temperature cross-sensitivity of FBG strain sensors embedded onto different substrates. Photonic Sensors, 13(1): 230127. https://doi.org/10.1007/s13320-022-0668-3
[33] Landreau, C., Morana, A., Ponthus, N., Le Gall, T., Charvin, J., Girard, S., Marin, E. (2023). Influence of adhesive bonding on the dynamic and static strain transfers of fibre optic sensors. Photonics, 10(9): 996. https://doi.org/10.3390/photonics10090996